

CHARACTERIZATION AND MELT SPINNING OF POLY (LACTIC ACID)/POLY (ETHYLENE GLYCOL) BLENDS

NUR ATIQA MOHD AKHIR¹, MAIZATULNISA OTHMAN¹
YOSE FACHMI BUYS², NORHASHIMAH SHAFFIAR¹, DZUN NORAINI JIMAT¹ AND
SHARIFAH IMIHEZRI SYED SHAHARUDDIN^{1*}

¹Department of Mechanical Engineering,
Kulliyah of Engineering,

International Islamic University Malaysia,
Jalan Gombak, 53100 Kuala Lumpur, Malaysia

²Department of Mechanical Engineering, Faculty of Engineering,
University of Malaya, 50603 Kuala Lumpur, Malaysia

*Corresponding author: shaimihezri@iium.edu.my

(Received: 15th February 2020; Accepted: 14th June 2020; Published on-line: 4th January 2021)

ABSTRACT: In this study, melt blended compositions of pure PLA with additions of polyethylene glycol (PEG) up to 30 wt% were prepared. Fourier-transform infrared spectroscopy (FTIR), differential scanning calorimeter (DSC), and thermogravimetric analysis (TGA) were used to investigate the properties of PLA/PEG blends, such as structural, thermal, and morphological properties. The results showed that further increments of PEG cause the -OH group of PLA/PEG blends to show a broad peak, indicating that there is hydrogen bonding interaction between PEG and PLA chains. DSC result revealed that the addition of PEG decreases the glass transition temperature from 57 °C to 46 °C and crystallization temperature from 107 °C to 87 °C. Such trends suggest enhanced chain mobility of PLA chains. TGA thermograms showed that further additions of PEG into PLA resulted in a consistent shift to lower temperature and decrease in thermal stability. Optical microscopy (OM) and scanning electron microscopy (SEM) observations of the melt spun PLA/PEG microfibers revealed that the diameter of the microfibers averaged between 15 to 80 microns.

ABSTRAK: Kajian ini menganalisa komposisi adunan lebur PLA asli bersama tambahan polietilena glikol (PEG) sebanyak 30%. Penjelmaan Fourier spektroskopi inframerah (FTIR), kalorimeter pengimbasan pembezaan (DSC) dan analisis termogravimetri (TGA) telah digunakan bagi mengkaji sifat-sifat adunan PLA/PEG, seperti struktur, terma dan sifat-sifat morfologi. Keputusan menunjukkan penambahan PEG seterusnya menyebabkan kumpulan -OH campuran PLA/PEG memberikan puncak yang lebar, ini menunjukkan ada interaksi ikatan hidrogen antara rangkaian PEG dan PLA. Keputusan DSC menunjukkan penambahan PEG mengurangkan perubahan gelas dari 57 °C kepada 46 °C dan suhu kristalisasi dari 107 °C kepada 87 °C. Trend ini mencadangkan peningkatan pergerakan rangkaian pada rangkaian PLA. Termogram TGA menunjukkan dengan penambahan berterusan PEG ke dalam PLA menghasilkan penurunan konsisten pada suhu dan pengurangan kestabilan haba. Pemerhatian mikroskop optik (OM) dan mikroskopi elektron penskanan (SEM) mikrofiber spun lebur PLA/PEG menunjukkan purata diameter mikrofiber ini antara 15 ke 80 mikron.

KEYWORDS: *microfiber; poly lactic acid (PLA); polyethylene glycol (PEG); melt spinning*

1. INTRODUCTION

The advancement of biodegradable polymers, particularly aliphatic polyester, has attracted curiosity and a great deal of interest among researchers due to their potentials as high performance biomedical and environment-friendly material [1,2]. Examples of aliphatic polyester are poly (lactic acid) (PLA), poly(glycolic acid) (PGA), and poly(caprolactone) (PCL) [3]. In recent years, PLA has received considerable attention due to biodegradability and biocompatibility properties [4]. PLA is one of the renewable resources that are rich in starch such as beetroots, corn, and potato [5] and allowed by the US Food and Drug Administration (FDA) for internal consumption [6,7].

PLA is a suitable candidate to be utilized for biomedical applications since the degradation product of PLA is non-toxic [8]. PLA possesses excellent mechanical properties and good physical properties such as high strength, thermoplasticity, and great processability [2,9]. There are various processing methods such as extrusion, injection molding, blow molding, thermoforming, and fiber spinning that PLA can go through to produce the desirable end product; solid shape, film, or fiber [13,14]. However, pure PLA has a stiff chain back-bone that restricts its plasticity [12] and causes low deformation at break and high modulus [13]. The stiffness of PLA can be improved by blending with other biocompatible plasticizers [14].

Plasticizer is used to increase flexibility and processability of matrix material [15]. Common examples of plasticizer are polyethylene glycol (PEG), polycaprolactone PCL, acetyl triethyl citrate and partial fatty acid esters [16]. In this study, polyethylene glycol (PEG) is used to improve PLA properties since it is non-toxic, miscible and biodegradable [17]. Phuphuak et al. [18] and Pillin et al. [19] stated that plasticizing PLA with PEG facilitates the chain mobility of PLA which results with improved ductility and drawability of the blends. Thus, these PLA/PEG blends can be melt spun into microfiber and potentially be used in biomedical application such as for wound dressings and sutures.

One of the manufacturing processes used to produce fibers is the melt spinning method. The melt spinning method does not require the use of solvents during the drawing process [20], is low in cost, and allows for continuous production of fiber [21]. The polymer material is melted into viscous liquid through the heater at the spinneret and then rapidly solidifies upon extrusion. In this paper, PLA and PEG were mixed at different compositions via melt blending method and were melt spun into microfiber.

2. MATERIALS AND METHODS

2.1 Materials

A pellet form of Poly (lactic acid) was purchased from Nature Works LLC (USA) grade 3052D Natureworks Ingeo TM Biopolymer. Polyethylene glycol flake was purchased from Merck (Darmstadt, Germany).

2.2 Preparation of PLA/PEG Blends

The PLA pellets were placed in a drying oven at 50 °C for an hour to remove moisture before being melt blended with PEG. The PLA/PEG compositions and their sample code are described in Table 1.

PLA, PEG, and PLA/PEG blends were mixed in an internal mixer (Haake PolyLab Rheomix) for 10 minutes at 170 °C mixing temperature with speed of 50 rpm. PLA, PEG, and PLA/PEG melt blended were then crushed using a crusher machine (HITOP, M SY-20)

into smaller pieces. The crushed PLA, PEG, and PLA/PEG blends acquired were then again dried in an oven for minimum an hour at temperature 50 °C to reduce the moisture contents.

Table 1: Composition of PLA/PEG blends sample used in this study

| Sample | Ratio (wt %) | |
|---------------|--------------|-----|
| | PLA | PEG |
| Pure PLA | 100 | 0 |
| 95/5 PLA/PEG | 95 | 5 |
| 90/10 PLA/PEG | 90 | 10 |
| 85/15 PLA/PEG | 85 | 15 |
| 80/20 PLA/PEG | 80 | 20 |
| 75/25 PLA/PEG | 75 | 25 |
| 70/30 PLA/PEG | 70 | 30 |
| Pure PEG | 0 | 100 |

2.3 Characterization of Melt Blended Compositions

2.3.1 Thermal property

a) Differential Scanning Calorimetry (DSC)

The thermal property test was conducted using a Sapphire DSC (Perkin Elmer Instruments, USA). The DSC was conducted for 2 samples for each composition that were measured in the range of 5–10 mg. Thermograms were obtained when the samples were heated at a temperature of 25 °C – 200 °C at a rate of 10 °C/min in a nitrogen environment. The glass transition temperature (T_g), crystallization temperature (T_c), melting temperature (T_m), melting enthalpy (ΔH_m), and crystallization enthalpy (ΔH_c) of the studied compositions were investigated. The crystallinity degree were also obtained based on Equation 1,

$$X_c (\%) = ((\Delta H_m - \Delta H_c) / \Delta H_o - W) \times 100 \% \quad \text{Equation (1)}$$

Where; ΔH_m = melting enthalpy of the PLA

ΔH_c = crystallization enthalpy of the PLA

ΔH_o = melting enthalpy of 100% crystalline PLA homopolymer 93.6 J/g [21]

W = wt % of PLA

b) Thermal Gravimetric Analysis (TGA)

TGA was conducted using a Simultaneous Thermal Analyzer (STA7300) (Hitachi High Technologies, USA) to determine the thermal property of the PLA, PEG, and PLA/PEG blends. The test was carried out under air atmosphere, heated at room temperature to 600 °C and a rate of 5 °C/min. The initial degradation temperature (T_i) and the final degradation temperature (T_f) were noted and investigated.

2.3.2 Structural Property

Fourier-Transform Infrared Spectroscopy (FTIR) was carried out using an FTIR spectroscopy Spectrum 100 (Perkin Elmer, USA) to characterize the presence and intensity of the functional groups of the studied compositions. The analysis was conducted in the range of 600 cm^{-1} to 4000 cm^{-1} with a resolution of 4 cm^{-1} and a scanning frequency of 16 per sample.

2.4 Melt Spinning and Characterization of PLA/PEG Microfiber

Microfibers of PLA/PEG were drawn using an in-house built melt spinning tower. The microfibers were spun at a spinning temperature of 150 °C – 160 °C and at a spinning speed of 430 rpm. An Olympus Microscope (BX41M, UK) was used to observe the diameter of the melt spun microfibers with a magnification of 20x. The fiber cross-sections were observed using a Scanning Electron Microscope (JEOL JSM-IT 100, Japan). The fiber samples were cut and placed on a double-sided carbon adhesive stub and coated with palladium using a Polaron SC7620.

3. RESULTS AND DISCUSSION

3.1 Fourier-Transform Infrared (FTIR) Analysis

Figure 1 shows the (FTIR) peaks of the PLA, PEG, and PLA/PEG blends. Table 2 represents the peak assignments and wave numbers for the samples.

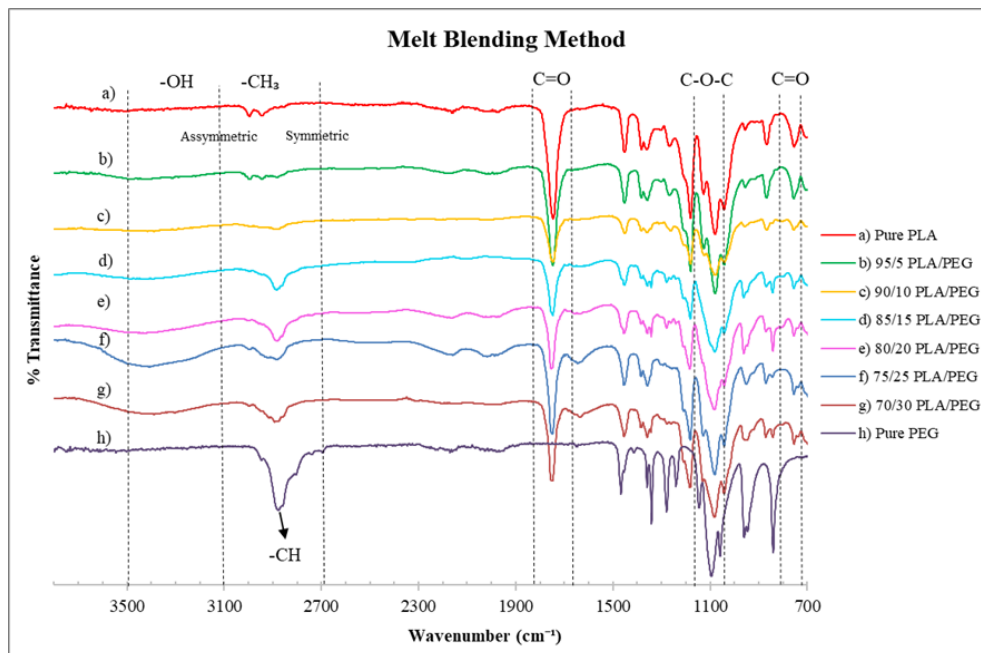


Fig. 1: FTIR spectra of various PLA/PEG blends used in this study.

Table 2: FTIR spectra of various PLA/PEG blends used in this study.

| Peak Assignment | Samples wavenumber (cm ⁻¹) | | | | |
|-----------------|--|--------------------------------|-------------------------------|-----------|-------|
| | -OH | -CH ₃ asymmetric | -CH ₃ symmetric | C=O | C-O-C |
| Pure PLA | 3503 | 2995 | 2942 | 1746; 754 | 1076 |
| 95/5 PLA/PEG | 3426 | 2993 | 2943 | 1747; 754 | 1078 |
| 90/10 PLA/PEG | 3388 | N/A | 2881 | 1747; 756 | 1078 |
| 85/15 PLA/PEG | 3427 | N/A | 2884 | 1747; 755 | 1077 |
| 80/20 PLA/PEG | 3440 | N/A | 2883 | 1754; 755 | 1077 |
| 75/25 PLA/PEG | 3409 | N/A | 2886 | 1749; 755 | 1080 |
| 70/30 PLA/PEG | 3388 | N/A | 2892 | 1754; 754 | 1084 |
| Pure PEG | 3466 | -CH stretching; 2879 | | N/A | 1095 |

The PLA backbone structure consists of the carbon chain of the carbonyl group (C=O) while PEG structural arrangement is made of C-O-C bonds. The IR spectra of the carbonyl group (C=O) of PLA appears at the frequency region of 754-756 cm^{-1} and 1746-1754 cm^{-1} . Meanwhile, for PEG, the C-O-C group appears at the frequency of 1095 cm^{-1} . The PLA showed peaks of the asymmetrical CH_3 and symmetrical CH_3 at 2995 cm^{-1} and 2942 cm^{-1} , respectively.

It was observed that as the incorporation of PEG increases above 10 wt %, the stretching for asymmetrical CH_3 became invisible (refer Table 2). The FTIR graph showed a strong methylene/methyl band (CH_2/CH_3) at 1470 cm^{-1} and a weak methyl band (1380 cm^{-1}), plus a band between 725-720 cm^{-1} (methylene rocking vibration). The presence of these bands indicates the existence of linear aliphatic structure in the form of long chains. This is attributed to the crystallinity and the formation of a backbone structure with a high amount of regularity in the PLA/PEG blends [22].

The spectra showed only one significant peak of the C-H stretching band. The peak that correlates to C-H stretching became more intense as the amount of PEG wt% increased. The PLA and PEG were melt blended at a temperature of 170 °C and a study by Sarasua et al. [23] suggested that such melt blending process may have resulted in a stronger C-H interaction. The presence of OH functional groups in the PLA structure was confirmed by the presence of a broad peak at 3422 cm^{-1} .

The C-H stretch vibrations for methyl ($-\text{CH}_3$) and methyne ($-\text{CH}$) in PLA and PEG structure, respectively confirm that both compounds are organic-based compounds that contain at least one aliphatic fragment or center. It can be seen that with further increments of PEG wt%, the incorporation of PEG increases, and the -OH group of PLA/PEG blends showed an increasingly broader peak. Thus, it is proposed that interaction of the hydrogen bonds between the two polymers [24,25] have occurred in the PLA/PEG blends. Similar observations were also deduced by Chieng et al. [9]. The author suggested [9] that the hydrogen bonding may have occurred due to intermolecular interaction between the oxygen that is fixed to the carbonyl (C=O) in PLA structure and the hydroxyl ($-\text{OH}$) terminal group present in the PEG molecular structure.

3.2.1 Differential Scanning Calorimetry (DSC) Analysis

The thermogram characteristics are shown in Figure 2 and information on glass-transition temperatures (T_g), crystallization temperatures (T_c), and melting temperatures (T_m) are tabulated and presented in Table 2.

Table 2: The thermal properties of various PLA/PEG compositions used in this study based on DSC analysis.

| Sample | T_g (°C) | T_c (°C) | H_c (J/g) | T_m (°C) | H_m (J/g) | X_c (%) |
|---------------|------------|-------------|-------------|-------------|-------------|-----------|
| Pure PLA | 57.3 ± 0.3 | 107.6 ± 0.7 | 31.5 | 155.3 ± 0.1 | 32.6 | 1.2 |
| 95/5 PLA/PEG | 46.3 ± 0.1 | 84.1 ± 0.1 | 21.8 | 152.8 ± 0.2 | 29.5 | 8.7 |
| 90/10 PLA/PEG | 44.9 ± 0.8 | 87.4 ± 0.1 | 21.2 | 151.5 ± 0.8 | 36.2 | 17.9 |
| 85/15 PLA/PEG | 40.1 ± 1.9 | 87.1 ± 0.2 | 16.5 | 152.7 ± 0.7 | 38.5 | 27.7 |
| 80/20 PLA/PEG | 40.5 ± 0.5 | 87.4 ± 1.0 | 13.9 | 151.8 ± 0.0 | 33.9 | 34.2 |
| 75/25 PLA/PEG | 38.5 ± 0.4 | 86.7 ± 0.4 | 1.3 | 151.5 ± 0.2 | 34.4 | 47.1 |
| 70/30 PLA/PEG | 37.0 ± 0.0 | 83.3 ± 0.3 | 3.7 | 151.6 ± 0.3 | 32.3 | 45.8 |
| Pure PEG | - | - | - | 67.6 | 175.9 | - |

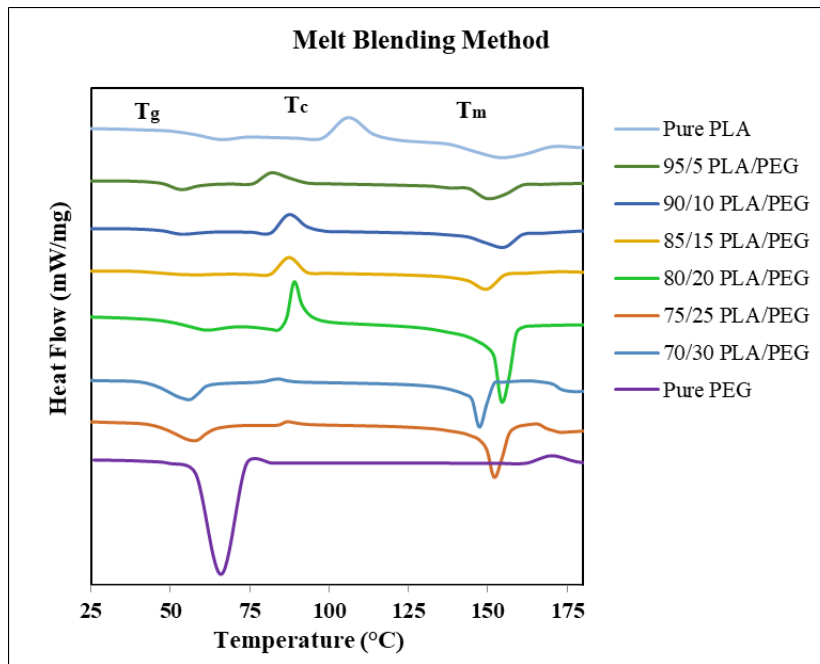


Fig. 2: Characteristics of DSC thermograms of various PLA/PEG compositions used in this study.

The T_g , T_c and T_m values of pure PLA are observed at 57 °C, 107 °C, and 155 °C, respectively. As PEG is added to PLA, the resultant PLA/PEG blends exhibited a trend of decreasing T_g values compared to pure PLA. The decreasing T_g trend with further PEG additions indicates enhanced chain mobility of PLA backbones [2,15,26]. Furthermore, PEG is formed based on a chain structure that allows greater degree of flexibility compared to the chain structure of PLA [16]. Thus, the PEG chains may be able to occupy the intermolecular spaces between PLA polymer chains to form hydrogen bonding [17,27]. The FTIR result (Figure 1) also showed a strong intensity correlated to hydroxyl bonding with further increments of PEG wt %. The decreasing T_g trend was also consistent with the studies by Hashim et al. [27] and Pivsa et al. [2].

The improved mobility of the blends with PEG addition facilitates the crystallization event to occur at lower temperatures. Moreover, Table 2 shows that the blend's crystallinity (X_c) increases as the concentration of PEG increases up to 25 wt % indicating that a good plasticization effect from PEG. However, as PEG was added at 30 wt %, the crystallinity of the PLA/PEG blend slightly decreased to 1.3%. A comparable trend of decreasing crystallinity degrees was also obtained by Li et al. [17] and was proposed due to the separation of the PEG phase in the blend. It is observed that the further increments of PEG into PLA decrease the melting temperature by 3-4 °C. A similar T_m trend was also observed by Chieng et al. [28].

3.2.2 Thermogravimetric Analysis (TGA)

The TGA was performed to identify the thermal properties of the studied compositions. Table 3 shows relevant data of the TGA thermogram for initial degradation temperature (T_i) and final degradation temperature (T_f) of these blends. The TGA thermograms of PLA, PEG, and PLA/PEG blends in the range of 40 °C to 450 °C are shown in Figure 3. It was observed that the studied compositions experienced a single weight-loss behavior. The T_i of pure PLA occurred at 323 °C. It is known that PLA has hydroxyl end groups in the main chain of its molecular structure. According to Song [29] and Maiza [26], hydroxyl end

groups will be critically affected during thermal degradation due to chain-scission which leads to decreasing thermal stability of PLA.

Table 3: The T_i and T_f obtained from TGA for various PLA/PEG compositions in this study

| Sample | T_i (°C) | T_f (°C) |
|---------------|------------|------------|
| Pure PLA | 323.3 | 384.1 |
| 95/5 PLA/PEG | 315.3 | 378.6 |
| 90/10 PLA/PEG | 308.5 | 374.4 |
| 85/15 PLA/PEG | 305.1 | 392.4 |
| 80/20 PLA/PEG | 306 | 383.3 |
| 75/25 PLA/PEG | 304.6 | 419.2 |
| 70/30 PLA/PEG | 301 | 433.6 |
| Pure PEG | 230 | 510 |

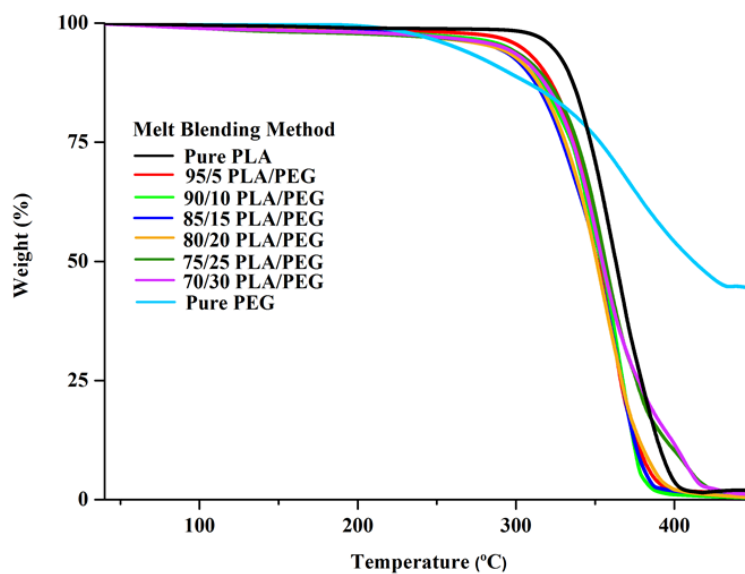


Fig. 3: TGA thermograms for various PLA/PEG compositions used in this study.

Pure PEG only experiences a weight loss of 60% as the temperature reaches 400°C and T_f at 510 °C. Comparable study by Zhang et al. [12] reported that PEG with different (high and low) molecular weight affects the thermal stability of a polymer blend and concluded that high molecular weight of PEG requires extra energy to undergo chain scission due to the longer chain thus indicates higher thermal stability. Septevani & Bhakri [30] and Silverajah et al. [31] proposed that the long polymer chain of PEG functioned as a surface protector of the polymer blends. The presence of the protective layer impedes the permeability of volatile degradation products out from the blend and slows down the degradation of the blend.

Further increments of PEG wt% into PLA resulted with a trend of decreasing T_i temperatures. Other studies have also observed similar trend [12,16]. According to Chieng et al. [28], PEG chains scatter themselves around PLA chains and break the polymer-polymer interactions that led to a decrease in thermal stability. It is necessary to identify the temperature region where thermal degradation will commence to avoid decrease in physical and mechanical properties at the melt spinning temperature for the studied compositions [31].

3.3 PLA/PEG Fibers

3.3.1 Morphological Study

The surface morphologies and diameter of melt spun fibers are depicted in the optical microscope (OM) micrographs at 20x magnifications in Fig. 4. Table 4 shows the average fiber diameter for the PLA and PLA/PEG fibers.

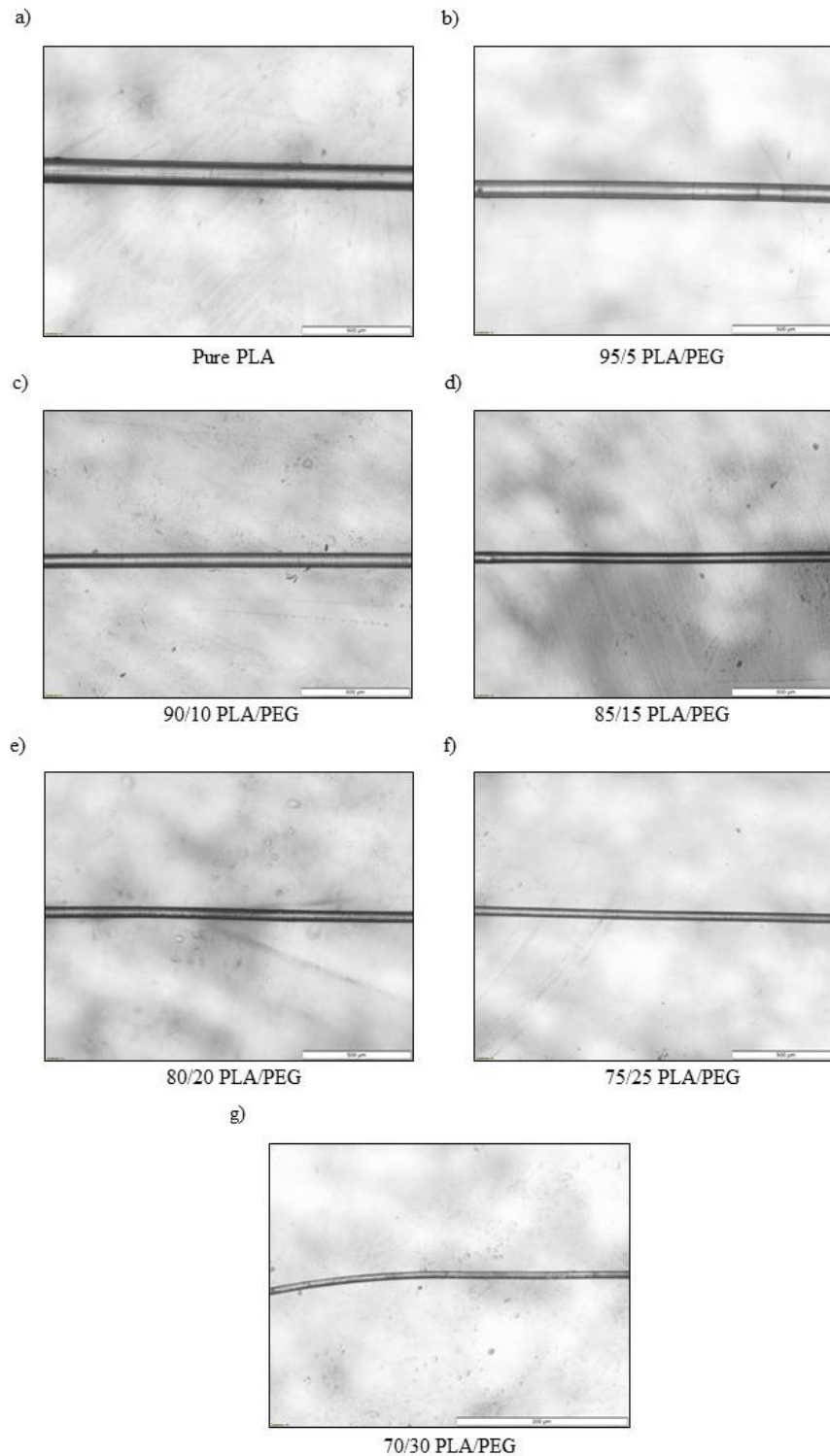


Fig. 4: OM micrographs of the melt spun microfiber for various PLA/PEG compositions used in this study.

It can be observed from Table 4 that the increase of PEG wt % led to a trend of decreasing fiber diameter from 112 μm to 15 μm . It was therefore deduced that the increase in chain mobility (as evidenced in DSC result) further reduced the viscosity of the PLA/PEG blends at the melt-spinning temperature of 150 $^{\circ}\text{C}$ – 160 $^{\circ}\text{C}$. This, in turn, exerted an increase in the degree of flexibility and workability [32] which enables much thinner fibers to be drawn. The OM images (Figure 4) revealed that the melt spinning process produces clear, bead-free, and uniform PLA and PLA/PEG microfibers. The surface and cross-section morphologies of PLA/PEG fibers are depicted in scanning electron microscopy (SEM) micrographs at 500x magnifications in Fig. 5.

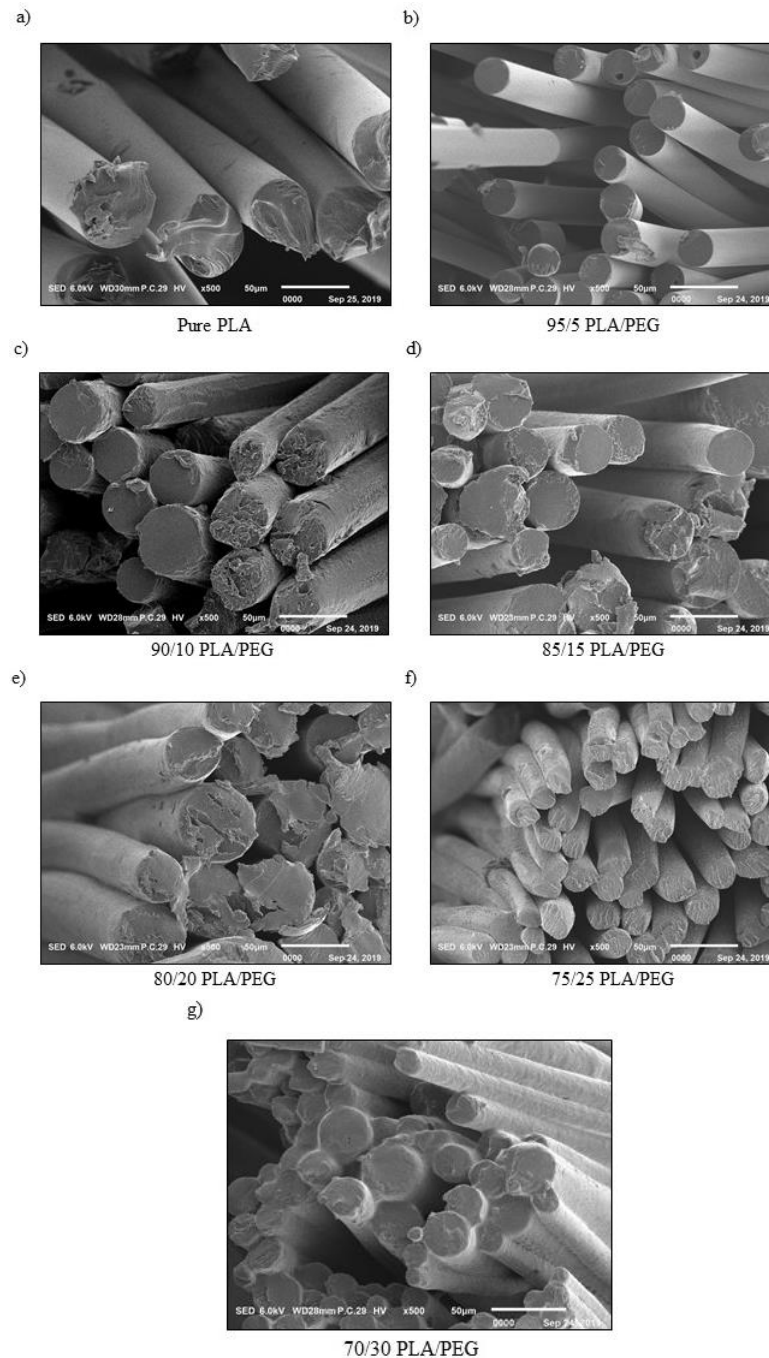


Fig. 5: SEM micrographs at 500x magnification of the melt spun microfiber for various PLA/PEG compositions used in this study.

Table 4: Measured diameter obtained via OM for the melt spun PLA/PEG microfiber

| Sample | Fiber diameter (μm) |
|---------------|----------------------------------|
| Pure PLA | 112 |
| 95/5 PLA/PEG | 80 |
| 90/10 PLA/PEG | 67 |
| 85/15 PLA/PEG | 60 |
| 80/20 PLA/PEG | 48 |
| 75/25 PLA/PEG | 38 |
| 70/30 PLA/PEG | 15 |

The SEM micrographs of melt spun PLA and PLA/PEG fibers at spinning temperature 150 °C – 160 °C revealed that all the fibers produced were circular cross-section in shape. PLA fiber has a smooth, uniform morphology, and larger fiber diameter than PLA/PEG fibers. With increasing PEG wt%, it was revealed that the surface of the fiber transitions from smooth to slightly rough. Such rough surface condition is proposed due to thermally induced phase separation of PLA and PEG. Mohamed [33] and Buttaro et al. [34] explained that the tendency for phase separation increases during melt spinning due to its processing conditions such as the distance from the spinneret to take-up wheels and the spinning temperature. Similar surface condition was also noted by Clarkson et al. [35] on microfiber produced via melt spinning method.

4. CONCLUSION

In this study, the effect of PEG addition was structurally and thermally characterized via FTIR, DSC, TGA, and SEM. FTIR results suggest that the intermolecular reaction occurring between hydrogen and oxygen and the carbonyl (C=O) in the PLA structure reacts with hydroxyl (–OH) terminal group in the PEG molecular structure. Such interactions were indicated by the increasing broad peak of –OH group as PEG composition in PLA/PEG blend increased. The crystallinity degrees of PLA/PEG blends showed increasing trend up to 25 wt % PEG indicating a good plasticization effect from PEG. TGA results revealed that the addition of PEG into PLA lowers the T_i and T_f of PLA/PEG. This is attributed to the poor thermal stability of PEG. The melt spinning method was then used to successfully produce bead-free and uniform PLA/PEG microfibers. The mechanical performance of these melt drawn fibers will be investigated in the next phase of this study.

ACKNOWLEDGMENT

This work was fully supported by the International Islamic University Malaysia, IIUM (RIGS17-052-0627). The authors would like to express their deepest gratitude to facilities and technical assistance provided by the International Institute for Halal Research and Training (INHART), IIUM.

REFERENCES

- [1] Farah TMN, Nadia AA. (2014) Study the mechanical and thermal properties of biodegradable polylactic acid/poly ethylene glycol nanocomposites. *International Journal of Application or Innovation in Engineering & Management*, 3(1): 459-464.
- [2] Weraporn P, Kazunori F, Keiichiro N, Yuji A, Hitomi A, Hideki Y. (2016) The effect of poly (ethylene glycol) as plasticizer in blends of poly (lactic acid) and poly (butylene succinate). *Journal of Applied Polymer Science*, 133(8): 1-10.

- [3] Mariya S, Olya S, Nevena M, Iliya R, George A. (2007) Preparation of PLLA/PEG Nanofibers by Electrospinning and Potential Applications. *Journal of Bioactive and Compatible Polymers*, 22(1): 62-76.
- [4] Gupta AP, Vimal K. (2007) New emerging trends in synthetic biodegradable polymers - Polylactide: A critique. *European Polymer Journal*, 43(10): 4053-4074.
- [5] Ching WL, Chun HY, Yueh SC, Tsung CH, Jia HL and Wen HH. (2008) Manufacturing and Properties of PLA Absorbable Surgical Suture. *Textile Research Journal* 78(11): 958-965.
- [6] Yangling C, Shaobo D, Paul C, Roger R. (2009) Polylactic acid (PLA) synthesis and modifications: A review. *Frontiers of Chemistry in China*, 4(3): 259-264.
- [7] Cynthia DCE, Ricardo JA, Jarbas MR, Roberto FSF and Ricardo GS. (2012) Synthesis and Characterization of Poly(D, L-Lactide-co-Glycolide) Copolymer. *Journal of Biomaterials and Nanobiotechnology*, 3: 208-225.
- [8] Lin X, Bo W, Guang Y and Mario G. (2006) Poly(Lactic Acid)-Based Biomaterials: Synthesis, Modification and Applications. In *Biomedical Science, Engineering and Technology*. Edited by Prof. Dhanjoo N. Ghista. InTech; pp 248-282.
- [9] Buong WC, Nor AI, Wan MZWN, Mohd ZH. (2014) Poly(lactic acid)/poly(ethylene glycol) polymer nanocomposites: Effects of graphene nanoplatelets. *Polymers*, 6(1): 93-104.
- [10] Jong-Whan R, Amar KM, Sher PS, Perry KWG. (2006) Effect of the processing methods on the performance of polylactide films: Thermocompression versus solvent casting. *Journal of Applied Polymer Science*, 101(6): 3736-3742.
- [11] Muhammad AAS, Wan AWAR, Rohah AM. (2014) Effect of different solvents on the thermal, IR spectroscopy and morphological properties of solution casted PLA / starch films. *Malaysian Journal of Fundamental and Applied Sciences*, 10(1): 33-36.
- [12] Jianming Z, Shiwei W, Yuhui Q, Qian L. (2016) Effect of morphology designing on the structure and properties of PLA/PEG/ABS blends. *Colloid and Polymer Science*. 294(11):1779–1787.
- [13] Hu Y, Rogunova M, Topolkaev V, Hiltner A, Baer E. (2003) Aging of poly(lactide)/poly(ethylene glycol) blends. Part 1. Poly(lactide) with low stereoregularity. *Polymer*, 44(19): 5701-5710.
- [14] Aswini KM, Smita M, Sanjay KN. (2014) Properties and characterization of biodegradable poly (lactic acid) (PLA)/poly(ethylene glycol) (PEG) and PLA/PEG/organoclay. *J. Thermoplast. Compos. Mater.*, 29(4): 443-463.
- [15] Savitha S, Girija B, Ravichandran K. (2018) Effect of Polyethylene glycol on Mechanical, Thermal, and Morphological Properties of Talc Reinforced Poly(lactic acid) Composites. *Materials Today: Proceedings*, 5(1): 1591-1598.
- [16] Saddys RL, Bernabe LR, Monica AP, Florence PS. (2012) Poly(ethylene glycol) as a compatibilizer and plasticizer of poly(lactic acid)/clay nanocomposites. *High Performance Polymers*, 24(4): 254-261.
- [17] Feng JL, Shui DZ, Ji ZL, Jun ZW. (2015) Effect of polyethylene glycol on the crystallization and impact properties of polylactide-based blends. *Polymer Advanced Technologies*, 26: 465-475.
- [18] Yupin P, Yong M, Philippe Z, Suwabun C. (2013) Balancing crystalline and amorphous domains in PLA through star-structured polylactides with dual plasticizer / nucleating agent functionality. *Polymer*, 54:7058-7070.
- [19] Isabelle P, Nicolas M, Yves G. (2006) Thermo-mechanical characterization of plasticized PLA: Is the miscibility the only significant factor? *Polymer*, 47(13): 4676-4682.
- [20] Nor AI, Wan MZWN, Maizatunisa O, Khalina A, Kamarul AH. (2010) Poly (Lactic Acid) (PLA)-reinforced kenaf bast fiber composites: The effect of triacetin. *Journal of Reinforced Plastics and Composites*, 29(7): 1099-1111.
- [21] Gupta VB, Kothari VK. *Manufactured Fibre Technology*, First Edit. Chapman & Hall, 1997.
- [22] Kurniawan Y, Yohanes AP, Setyo P, Bruce AW, Hadi KP, Titi CS. (2016) Infrared and Raman studies on polylactide acid and polyethylene glycol-400 blend. *AIP Conference Proceedings*. 1725, 020101.
- [23] Jose-Ramon S, Nerea LR, Alberto LA, Emilio M. (2005) Stereoselective crystallization and specific interactions in polylactides. *Macromolecules*, 38(20): 8362-8371.

- [24] Yong J, Xin-Yao Y, Tao L, Mei-Yun Z, Jin-Huia L, Xing-Jiu H. (2013) PEG aggregation templated porous ZnO nanostructure: Room temperature solution synthesis, pore formation mechanism, and their photoluminescence properties. *CrystEngComm.*, 15(18): 3647-3653.
- [25] Decai L, Yang J, Shanshan L, Xiaojing L, Jiyou G, Qifeng C, Yanhua Z. (2018) Preparation of plasticized poly (lactic acid) and its influence on the properties of composite materials. *PLoS One*, 13(3): 1-15.
- [26] Mounira M, Mohamed TB, Guilhem Q, Valerie MN. (2015) Biobased additive plasticizing Polylactic acid (PLA). *Polimeros*, 25(6): 581-590.
- [27] Norazlina H, Kamala R, Santhoshini S, Kamal Yusoh. (2015) Effect of Processing Method on Thermal Behavior in PLA/PEG Melt Blending. *Advanced Materials Research*, 1134: 185-190.
- [28] Buong WC, Nor AI, Wan MZWN, Mohd ZH. (2013) Plasticized Poly (lactic acid) with Low Molecular Weight Poly (ethylene glycol): Mechanical, Thermal and Morphology Properties. *Journal of Applied Polymer Science*, 130(6): 4576-4580.
- [29] Yan PS, De YW, Xiu LW, Ling L, Yu ZW. (2011) A method for simultaneously improving the flame retardancy and toughness of PLA. *Polymer advanced technologies*, 22(12):2 295-2301.
- [30] Athanasia AS, Samsul BI. (2017) Plasticization of poly (lactic acid) using different molecular weight of poly (ethylene glycol). In *Proceedings of the 3rd International Symposium on Applied Chemistry: 23–24 October 2017; Jakarta, Indonesia. Volume 1904. Issue 1.*
- [31] Giita S, Nor AI, Norhazlin Z, Wan MZWY and Hazimah AH. (2012) Mechanical, thermal and morphological properties of poly(lactic acid)/epoxidized palm olein blend. *Molecules*. 17(10): 11729–11747.
- [32] Melissa GAV, Mariana AS, Lucielen OS, Marisa MB. (2011) Natural-based plasticizers and biopolymer films: A review. *European Polymer Journal*. 47(3):254–263.
- [33] Khayet M. (2015) Melt Spinning. *Encyclopedia of Membranes*.
- [34] Larissa. MB, Erin D, Margaret WF. (2014) Phase separation to create hydrophilic yet non-water soluble PLA/PLA-b-PEG fibers via electrospinning. *Journal of Applied Polymer Science*, 131(19): 1-7.
- [35] Caitlyn MC, Sami MEAA, Reaz C, Shoumya NS, James S, Gregory S, Volkan O, Jeffrey PY. (2019) Melt Spinning of Cellulose Nano fibril/Polylactic Acid (CNF/PLA) Composite Fibers for High Stiffness. *Applied Polymer Material*, 1:160-168.